FERMILAB-PUB-20-540-DI-TD

Flexible linkages for thermal management at cryogenic temperatures

R. C. Dhuley

Fermi National Accelerator Laboratory, Batavia IL, 60502

1. Introduction

Cryogenic system design often presents the competing requirements of thermal coupling between components while de-coupling them structurally. Good thermal coupling is necessary for adequate thermal management during cryogenic operation of the system and to reduce the cooldown time from the ambient to cryogenic temperature. Structural de-coupling is essential to reduce thermal stresses during cooldown, mitigate the trasmission of vibration and loads to sensitive and/or fragile components, and compensate for integration misalignments. Flexible thermal links (FTLs) are an essential component of cryogenic systems that provides a balance between thermal coupling and structural isolation.

FTLs typically have a middle flexible-conductor (FC) connected at its ends to two rigid end-connectors (ECs). The ECs provide for integration of the FTL with the components to be coupled. Flexibility in an FC is achieved by stacking together thin foils or bundling together strand-woven cables of a thermally conducting material. These processes produce a foil FTL or a cable FTL respectively.

Bugby and Marland [1] have given an excellent review of foil and cable FTLs constructed for aerospace cryogenic applications. This covers typical requirements, construction methods, and thermal and mechanical charateriation techniques. Since this review of 2003, there has been growing interest in the use of lightweight carbon-based materials for FTLs and the development of FTLs for temperatures below that of liquid helium down into the sub-Kelvin regime. The intent of this chaper is to discuss these developments and offer the reader some guidelines for FTL material selection, construction, and thermal characterization. The first part of the chapter deals with the choice of material for FC. Examples of investigations are given that use FC materials sourced from commercial vendors. In the second part, examples of thermal link manufacturing methods are presented including those that make the FTLs usable at sub-Kelvin temperatures. The third part discusses thermal conductance characterization methods. Finally, usage examples of FTLs are decsribed for emerging applications.

2. Material Selection for FTL Flexible Conductor

Key functionality of an FTL is to provide the required thermal conductance (heat flow rate/temperature difference) and flexibility with a size and weight as small as practical. Therefore, the relevant properties for selecting a material for an FTL are thermal conductivity, k , modulus of elasticity, E, and density, ρ. Often, the ratios k/E and k/ρ are considered as figures of merit for an FC material. The material with higher ratios is considered superior. In this section, we look at these properties for some FTL FC materials. As thermal conducivity of materials is highly dependent on temperature in the cryogenic range, the discussion is divided into two subsections: T > 50 K and T < 50 K.

2.1 Thermal links for 50 – 300 K

This warmer cryogenic temperature range is of interest to cryocooler conduction-cooled HTS devices, radiatively cooled electronic systems onboard spacecrafts, infrared sensors, and other near room temperature cooling applications. Thermal conductivity of four common FC materials for use in this temperature range are compared in figure 1. These include carbon based pyrolitic grapite sheet (PGS) [2,3], graphite fiber K1100 [4], and the metals aluminum and copper [5].

The great appeal of carbon based PGS and graphite fiber K1100 comes from not only their significantly higher thermal conductivity than of the metals, but also their much lower density. Both the PGS and K1100 are 20-30% lighter than aluminum. Consequently, k/ρ for PGS and K1100 is respectively >10 and >2.5 times that of aluminum near 150 K. Therefore, above 50 K, a carbon composit FTL can offer much larger thermal conductance than a metallic FTL of same size and mass. This is attractive particularly for spaceflight applications.

Constructing FTLs using carbon composits, however, has several challenges. The most predominant challenge arises from the anisotropy in thermal conductivity. While the in-plane/along-the-fiber conductivity can be as high as that shown in figure 1, the out-of-plane conductivity is nearly a hundred-fold smaller. This low out-of-plane conductivity can restrict the flow of heat into the foil/fiber, thereby lowering the overall thermal conductance of an FTL. The high elastic modulus of carbon based conductors neccesiates making very thin (~0.01 mm) foils/fibers so that their stack/bundle achieves good flexibility. The high elastic modulus may also limit the utility of carbon based FTLs in applications where a large bend radius is required. Another known issue with graphite fiber FTL is that fibers tend to break and separate from the bundle, causing particulate contamination (this, however, can be addressed by specialized FTL manufacturing and quality control techniques [6]). If carbon composits are not feasible, the next choice of FC for lightweight applications is aluminum. Although its thermal conductivity is roughly 60% of copper, its three-fold smaller density results in larger thermal conductance for a given mass and size of the FTL. Furthermore, aluminum’s elastic modulus is nearly half of copper’s, which can produce FTLs of higher flexibility for same foil thickness or strand diameter. Therefore, aluminum FTLs offer larger k/E and k/ρ than copper for use above 50 K.

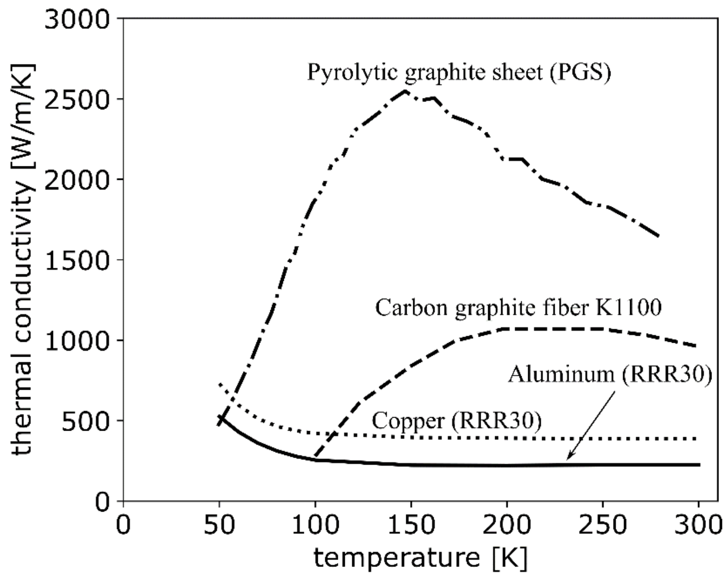

Figure 1. Comparison of thermal conductvity of materials for 50 – 300 K FTLs: pyrolytic graphite sheet (PGS) [2,3], K1100 [4], aluminum and copper [5]. Notes about PGS: (1) the thermal conductivity shown for PGS is in-plane; out-of-plane conductivity can be nearly a hundred-fold smaller, (2) the PGS shown is in its "uncompressed" brittle form and requires compression before it becomes flexible like paper; compressed PGS has slightly lower thermal conductivity than umcompressed PGS, (3) the PGS shown here is 10 µm thick; thermal conductivity is thickness dependent and is larger for thinner PGS.

2.2 Thermal links for <50 K

Thermal links below 50 K cater to applications such as cryocooler conduction cooling of MgB_2 and LTS (NbTi, Nb_3Sn) magnets, fast cooldown of large thermal masses present in astronomy experiments (dark matter search, gravitational wave detectors, telescope focal planes), and millikelvin systems (dilution refrigerators, adiabatic magnetization refrigerators, etc.) For this range, thermal conductivities of aluminum and copper of several purity grades are plotted in figure 2. The purity range is denoted in terms of conveniently measurable residual resistivity ratio or RRR, spanning 30 – 10000 for aluminum and 30 – 3000 for copper. These RRRs can be achieved by either annealing the metals or sourcing them from specialty metals suppliers. Comparing with the carbon composites, the metals have immensely greater thermal conductivity below 50 K making them suitable for FTLs for use at these temperatures. Thermal conductivity wise, both pure aluminum and copper are viable for temperatures down to about 1.2 K. Aluminum has notable advantages of being lighter, less sensitive to strain (often encountered when FTL are deformed excessively during operation), and is capable of self-annealing at ambient temperature in air [7] (for instance, after an unintentional deformation during construction of an FTL). There are, however, two disadvantages to aluminum – first, it becomes a superconductor below 1.2 K and rapidly loses its thermal conductivity and second, its surface is prone to carry notoriously hard oxide layer, which can produce large thermal contact resistance at low temperatures. Copper, on the other hand, continues to be a normal metal down to arbitrarily low temperatures and its surface oxide is easier to clean. Specifically, copper is the only thermally conducting material available for constructing FTLs for use below 1 K.

The reader is directed to the exhaustive reviews by Woodcraft [8] and Pobell [7] for discussions of thermal conductivity of aluminum and copper for varying degree of purity, effect of strain, and annealing. In what follows, a few examples are presented from researchers who have characterized commercial samples of high purity aluminum and copper for developing low temperature FTLs. To aid comparison, the measured data are overlaid in figure 2 on the reference data for aluminum and copper.

- Cu-1: Dhuley et al. [9] at Fermilab characterized a copper strand-woven cable sourced from Technology Applications (TAI), Inc. for developing FTLs to conductively couple a 10 mK dilution refrigerator to a 15 mK cryostat for dark matter search. An as-supplied cable sample showed RRR of 77; its equivalent thermal conductivity is plotted in figure 2. The cable sample is shown in figure 3.
- Al-1: At Fermilab, 5N aluminum foils of 0.5 mm thickness where characterized for developing FTLs for cryocooler conduction cooling of superconducting radiofrequency accelerator cavities near 4 K [10]. The samples sourced from Laurand Associates showed nearly 2000 W/(m*K) at 4.5 K without any heat treatment or annealing.
- Cu-2 and Cu-2a: These denote 0.8 mm thick 5N copper foils measured by Kimball and Shirron [11,12] at NASA Goddard Space Flight Center for developing thermal straps to be deployed on a spaceflight adiabatic demagnetization refrigerator. The samples sourced from ESPI Metals displayed RRR of 200 and 1045 before and after vacuum annealing. Details of the annealing process are given in figure 6.
- Al-2: Yamada et al. [13] developed flex links by bundling 0.15 mm diameter wires of 5N aluminum for cooling the KAGRA, a laser interferometer based gravitational wave detector in Japan. The primary twist has seven wires and the final bundle, shown in figure 3, is made by twisting together seven primary twists. The wire was sourced from Sumitomo Chemicals Ltd. The bundle was vacuum annealed for 3 hours at 450 ^{0}C, which resulted in thermal conductivity as high as 18500 W/(m*K) at 10 K (see figure 2 for the temperature dependence). Interestingly, Yamada report that there was no loss of RRR due to the possible strain arising during the bundling process (RRR remained close to 3100 before and after bundling). However, there was significant drop in RRR after the completed bundle was strained by winding around a 10 mm diameter cylindrical rod.
- Cu-3 and Cu-3a: Risegari et al. [14] measured 75 µm thick foils of OFHC copper between 30 – 150 mK for use in the CUORICINO experiment. The foils were sourced from Goodfellow and thermal conductivity was measured before and after vacuum annealing for 12 hours at 450 ^{0}C. After annealing, the thermal conductivity at 100 mK increased from 7 W/(m*K) to 17 W/(m*K).

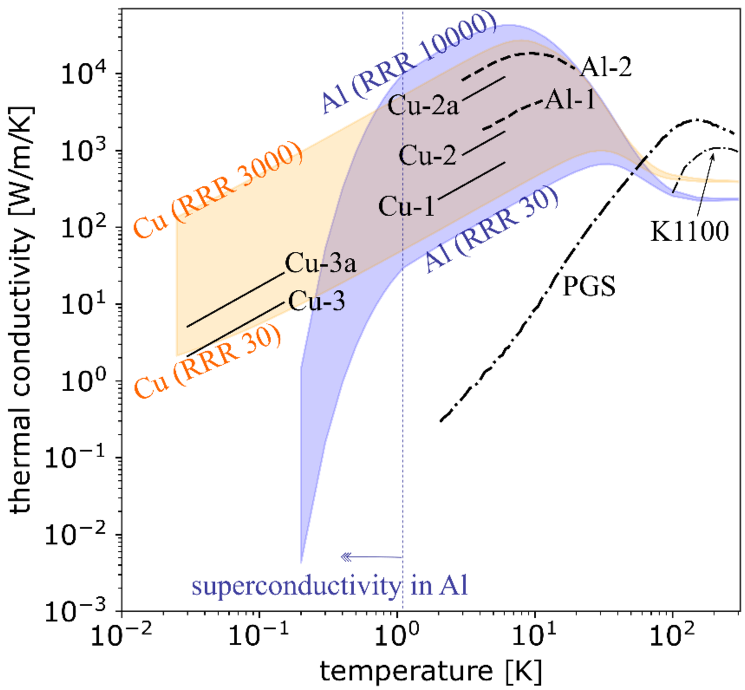

Figure 2. Reference thermal conductivity of copper and aluminum [5] showing the dependence on temperature and residual resistivity ratio (RRR). The aluminum data in the superconducting state below 1.2 K are estimated using the expression given by Woodcraft [8]. Overlaid on the reference data are experimental data measured by researchers who prepared in-house FTLs: (1) Cu-1: Fermilab measurement [9] of an OFHC strand-woven cable supplied by Technology Applications, Inc. (2) Cu-2: NASA GSFC [12] 5N 0.8 mm copper foil sourced from ESPI Metals before annealing (3) Cu-2a: NASA GSFC 5N copper foil after annealing (see figure 6 for annealing steps) (4) Cu-3: 75 um thick foil of OFHC copper from Goodfellow measured by Risegari et al. [14] before annealing (5) Cu-3a: Risegari's foil after vacuum annealing at 450 ^{0}C for 4 hours (6) Al-1: Fermilab measurement of 0.5 mm 5N aluminum foil supplied by Laurand Associates and (7) Al-2: Yamada et al. [13] measurement of cabled wire (0.15 mm diameter) rope of 5N aluminum supplied by Sumitomo Chemicals Ltd. Data for PGS [2,3] and K1100 carbon fiber [4] are shown for comparison.

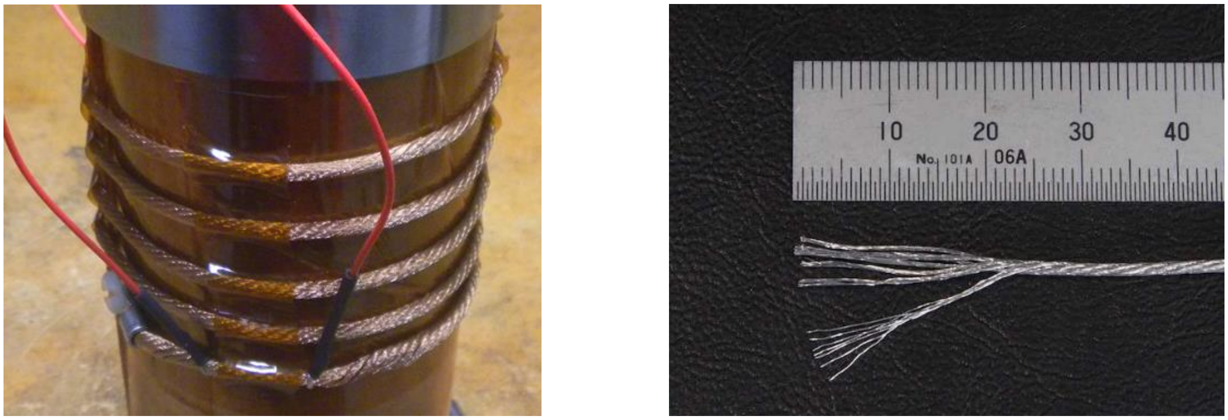

(a) (b)

Figure 3. (a) OFHC copper strand-woven cable made by Technology Applications, Inc. while being measured at Fermilab [9] (b) twisted-wire cable of 5N aluminum developed by Yamada et al. [13].

3. End-connector Attachment

After reviewing thermal conductivity of flexible conductors (FCs), we now look at methods for attaching the end-connectors (ECs) to the FC. The ECs provide structural interfacing of the FTL with components that are to be coupled. The connection between the FC and ECs must ensure minimal loss in flexibility and addition of only a small thermal resistance at the FC-EC contact.

PGS FCs are usually pressed between aluminum terminal blocks by swaging as pictured in figure 4 [15]. The end blocks are parallel slotted to increase the surface contact area between the foils and EC. After inserting the PGS into the slots, the slots are pressed to obtain a mechanical bond. Trollier's PGS FTL constructed following this method gave thermal conductance of 1.1 W/K at 110 K with a mass of <50 gm. Another method to bond PGS to ECs is by application of solders such as S-bond [16]. This solder enables bonding PGS to not only metallic ECs but also metal composites, silicon, and glasses. The FC-EC contact resistance imparted by the solder is not known for the cryogenic temperature range.

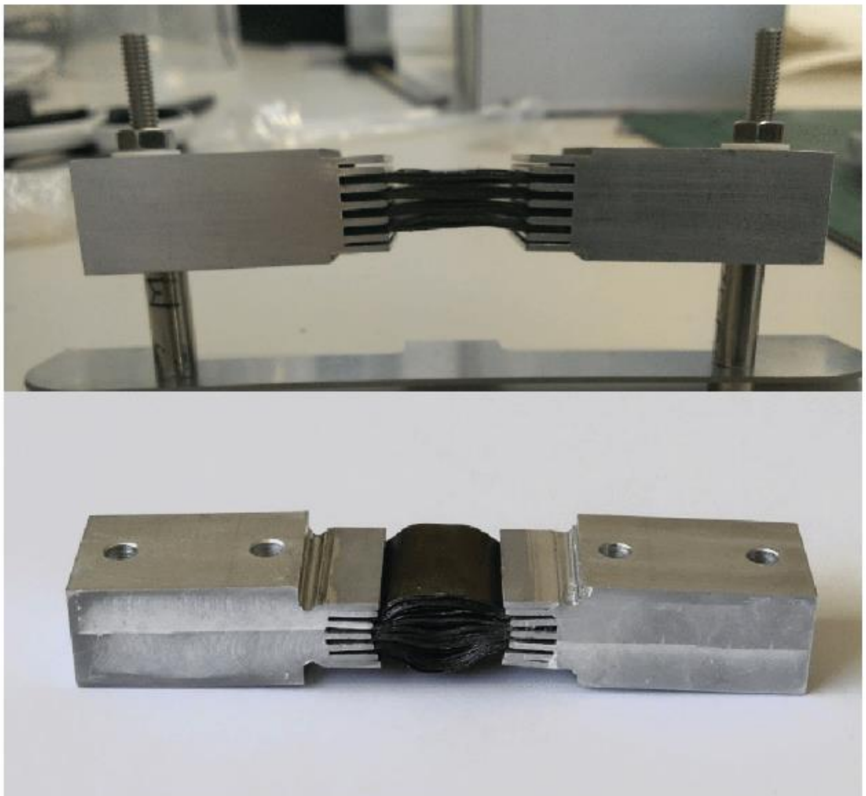

Figure 4: Thermal link produced by Trollier et al. [15] by swaging stacks of PGS between slotted Al1080 end-fittings.

Trollier et al. [15] have compiled details of a number of methods for making metallic FC – metallic EC connections. These are given in Table 1.

Table 1: FC-EC connection methods, their feasiblity, and the expected effect on FTL thermal performance [15].

Process available for foil assembly	**Aluminum foils and aluminum fittings**	**Copper foils and copper fittings**	**Copper foils and aluminum fittings**
TIG/MIG	Good but not critical on foils	Good	Not feasible
Press welding	Not feasible	Very good no thermal resistance between foils	Not feasible
Diffusion welding	Feasible with force applied during process	Good no deformation and good performances	Feasible with force applied during process
Laser welding	Feasible but spot welding only		Not feasible
Electron-beam welding	Very good no thermal resistance between foils		Not feasible
Brazing	Good with additional thermal resistance		
Swaging	Good with additional contact resistance between foils		

Trollier et al. [15] constructed thermal links of copper foils and aluminum foils using FC-EC joining processes from Table 1. Electron beam welding was chosen for fusing together 5N aluminum foils to Al1080 aluminum fittings to obtain low thermal contact resistance at the connection. After e-beam welding, the bulky end-fittings were machined to their final design. The process resulted in links of thermal conductance 0.5-0.9 W/K in the 50-70 K temperature range. For making the copper thermal link, a stack of OFHC copper foils was placed between two copper plates, pressure was applied, and electric current was passed through the contact area to heat it to 965 ^{0}C and fuse the foils with the copper plates. The process was performed under inert gas environment to prevent oxidation of copper. The EC was then machined to its final shape. The FTLs after post-production qualification and acceptance testing are displayed in figure 5.

Figure 5: Aluminum and copper foil straps produced by Trollier et al. [15] for 50-80 K space applications.

Kimball and Shirron [11] describe a process for constructing an OFHC copper foil FTL that was deployed on a spaceflight adiabatic demagnetization refrigerator. Eight foils of 0.8 mm thickness (source from ESPI Metals) were stacked, pressed with 3 MPa pressure using special fixtures, and heat treated in a vacuum environment. The heat treatment served to diffusion bond the foils at their end (resulting into low thermal contact resistance between the foils) and to anneal the foils. The annealing temperature profile shown in figure 6 raised the foil RRR from 200 to 1045 [12]. The resulting FTL had 0.6 W/K thermal conductance at 5 K. Figure 6 also shows the FTL after annealing and gold plating.

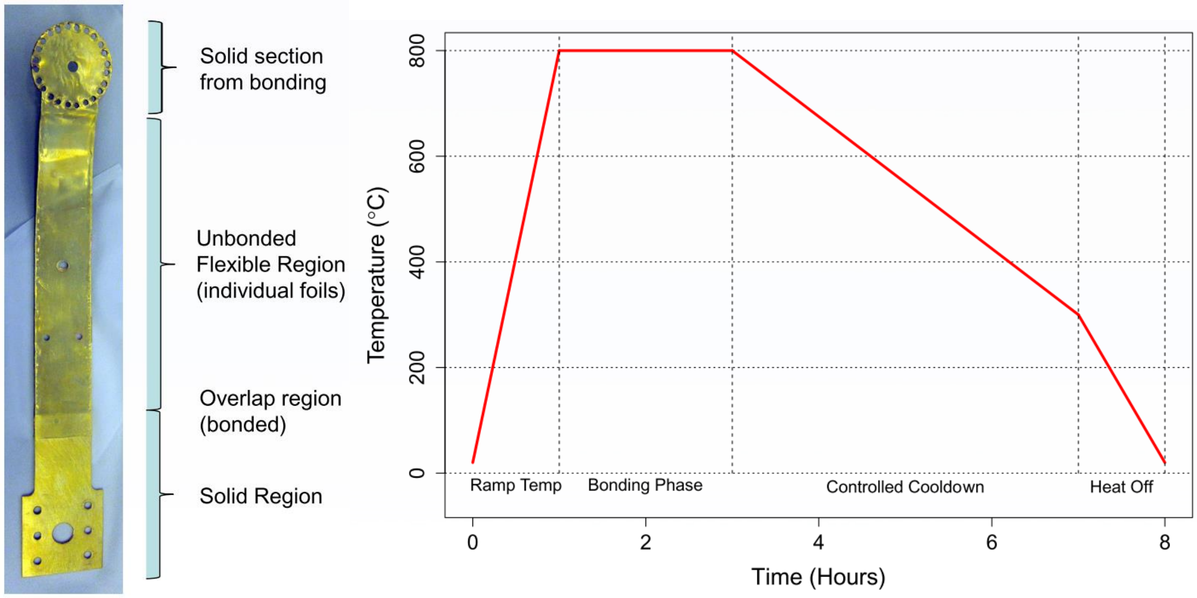

Figure 6: OFHC foil FTL made at NASA GSFC for spaceflight ADR heat switch operation – (left) the FTL with diffusion bonded terminations and (right) temperature-time profile for diffusion bonding and annealing the OFHC foils [11].

An off-the-shelf FTL from Technology Applications, Inc. was modified at Fermilab for use with the SuperCDMS cryostat to be operated near 15 mK [9,17]. The off-the-shelf FTL has UltraFlex copper cables (the FC) mechanically pressed into slotted OFHC copper ECs. Although effective at warmer temperatures, the mechanical FC-EC joints showed significant thermal resistance below 2 K. To reduce this resistance, the FC and EC were fused together by electron beam welding. As depicted in figure 7, an e-beam (voltage 50 kV, current 110 mA, speed of beam pass 40 inch/min) was passed across the width of the EC with full penetration into the EC thickness. The resulting fusion lowered the contact resistance significantly as determined from in-house thermal conductance measurements. As shown in figure 8, the unwelded FTL thermal conductance below ~2 K scaled as T^2, indicating a mechanical FC-EC contact containing surface oxide of copper. After welding, the scaling relation became T^1, representative of pure metallic thermal conduction. The thermal conductance of the welded FTL is 0.02 W/K at 130 mK, which is 70% of its theoretical value calculated from the cable RRR of 77. A plausible (but unconfirmed) reason for this deviation is that the extent of fusion may not be 100% (some FC strands may have remained unfused with the EC). Although the e-beam parameters need fine tuning to achieve 100% fusion, the technique is deemed effective for adapting off-the-shelf copper cable FTLs for sub-Kelvin applications.

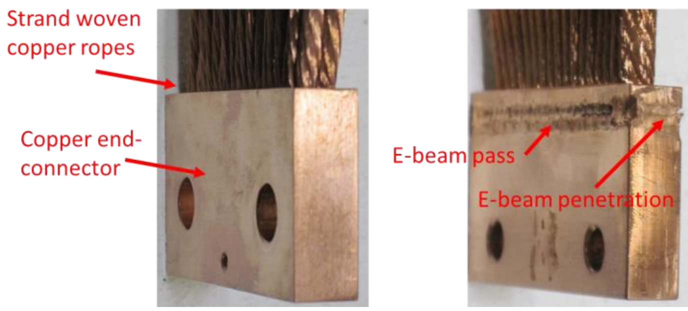

E-beam parameters	
Accelerating voltage	50 kV
Beam current	110 mA
Speed of pass	40 inch per minute

Figure 7. End-connector of a Technology Applications, Inc. UltraFlex copper strap: (left) as-purchased FTL with OFHC cables mechanically pressed in the EC, (center) the EC after an electron-beam pass (taken from [9]), and e-beam welding parameters (right).

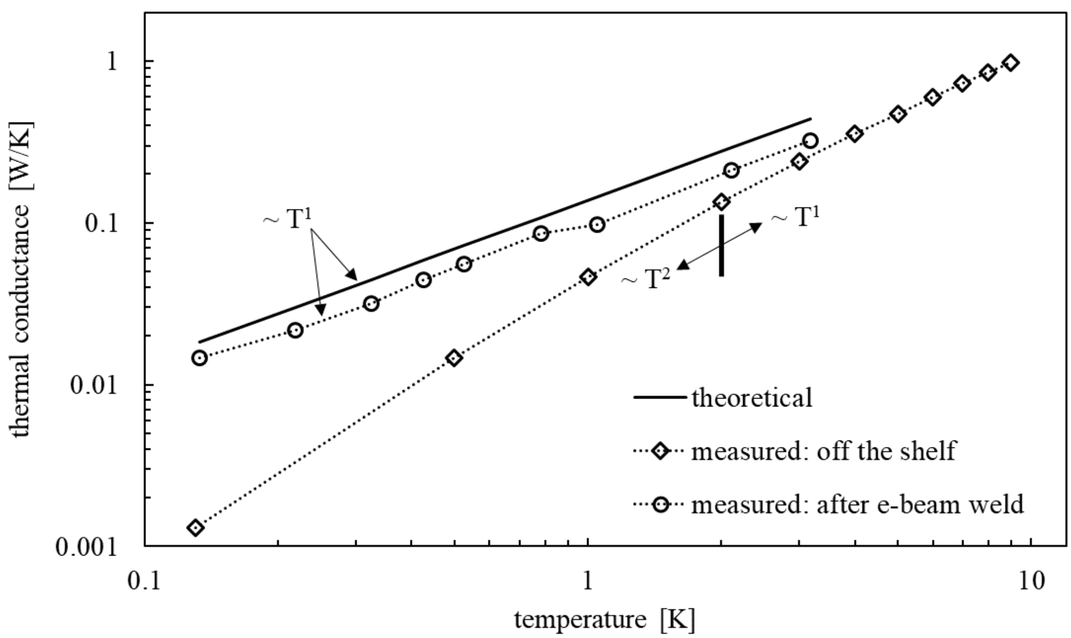

Figure 8: Thermal conductance of a Technology Applications, Inc. UltraFlex copper strap before and after e-beam welding of the ECs.

4. Thermal Characterization Techniques

The most common technique for cryogenic thermal conductance measurement of an FTL uses a steady state heat flow. The technique has two thermodynamically-equivalent variants as depicted in figure 9. Here an FTL is mounted from one of its ECs to a refrigerator cold plate (a cryocooler, ADR, or dilution refrigerator depending on the temperature range of interest). The assembly is enclosed in multilayer insulation (MLI) and cooled in a high-vacuum chamber ($<10^{-6}$ torr) to reduce parasitic heat leak. In figure 9(a), thermometers are placed on the two FTL ECs. The EC farther from the cold plate is equipped with a heater. During a test, the heater is powered with a heat flow, Q and temperatures, T_H and T_C are noted at steady state. FTL thermal conductance at $T_{avg} = 0.5*(T_C + T_H)$ is then calculated as $K_{FTL} = Q/(T_H - T_C)$. To capture an accurate temperature dependence of K_{FTL}, the temperature difference $T_H – T_C$ should be 1-2% of T_{avg}. Figure 9(b) shows the so-called 'two-heater' method wherein two heaters are used, one on each EC. Note that there is only one thermometer, on the farther EC. A measurement is done in two steps:

a. Power $Q_H = Q$ and keep $Q_C = 0$, measure $T_H = T_a$ at steady state

b. Keep $Q_H = 0$ and power $Q_C = Q$, measure $T_H = T_b$ at steady state

Thermal conductance at $T_{avg} = 0.5*(T_a + T_b)$ is then calculated as $K_{FTL} = Q/(T_a – T_b)$. Once again, $T_a – T_b$ should be 1-2% of T_{avg} to capture accurate temperature dependence of K_{FTL}. The two-heater method is useful particularly at very low temperatures (<1 K) because of two reasons: (1) the overall accuracy is improved because the temperature difference is obtained from just one thermometer and so the systematic uncertainty is small and (2) the cost of measurement is reduced since only one accurate cryogenic thermometer is required (calibrated low temperature thermometers are expensive compared to heaters).

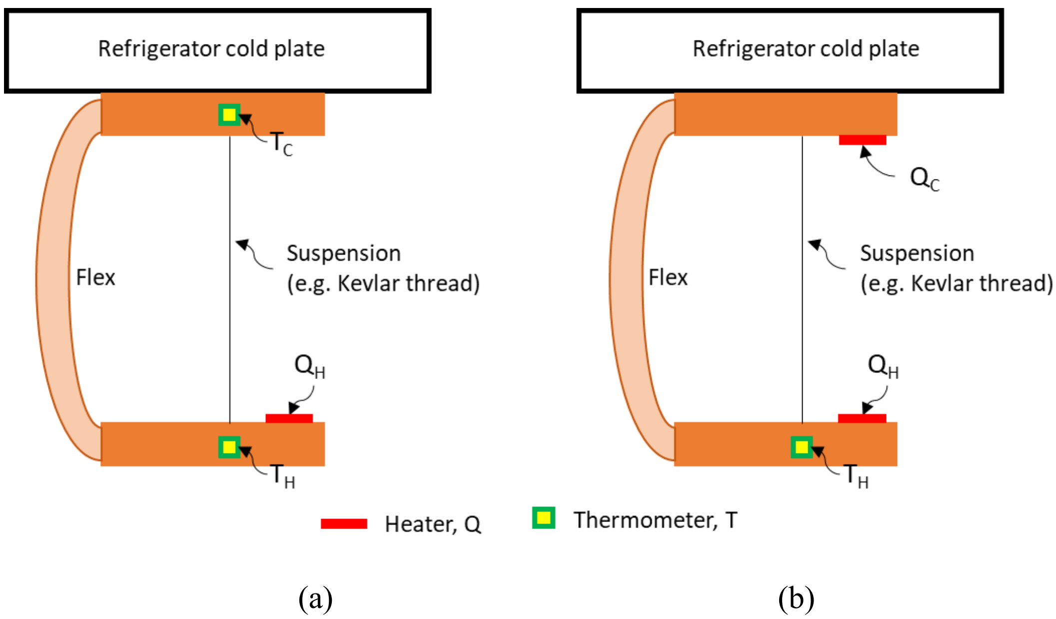

Figure 9. Longitudinal heat flow method for thermal conductance measurement of an FTL following (a) the steady-state longitudinal heat flow method and (b) the two-heater one-thermometer method.

In the case of metallic flexible links (welded or fused end-connections), a quick estimation of the thermal conductance near 4 K can be made from the residual resistance ratio (RRR). Thermal conductance, K_{FTL} is estimated using Wiedeman Franz law:

$$K_{FTL}(T) = L_0*T*(RRR/R_{FTL,RT}) \quad (1)$$

where T = ~4 K, L_0 is Lorenz number, $R_{FTL,RT}$ is electrical resistance of the FTL measured at room temperature. The Wiedeman Franz law is valid where the thermal conductivity is due to the electron channel (phonon channel is much smaller). This holds for pure aluminum and copper near liquid helium temperatures. The reader is cautioned to check the validity of Wiedeman Frank law for the link material and the temperature range of their interest before adopting this characterization technique.

5. Integrating the FTL with Cryosystems

FTLs are integrated with cryosystems most commonly by bolting their ECs to the system components. Such bolted contacts facilitate easy assembly/disassembly but introduces thermal resistance. Techniques to reduce this contact resistance include interposing the contact with indium, galinstan [18], and Apiezon N grease. The contacting surfaces can be gold plated if the use of thermal interface materials is not feasible. The reader is referred to the reports by Gmelin et al. [19] and Dhuley [20,21] for more details on thermal contact resistance at cryogenic temperatures.

6. Examples of Emerging Applications of FTLs

a) Sub-Kelvin cryostat for cryogenic dark matter search

The SuperCDMS SNOLAB experiment for dark matter search will use silicon and gemanium detectors operating at temperatures close to absoloute zero. The baseline design of the detector housing and its cryocooling scheme designed at Fermi National Accelerator Laboratory is depicted in figure 10. The housing comprises of a six-layered cryostat with the inner three layers operating at 1 K (ST layer), 250 mK (CP layer), and 15 mK (MC layer). A dilution refrigerator about ~10 feet away will conduction-cool the sub-Kelvin cryostat layers using tubular OFHC copper stems (called C-stems). The specified operating temperatures, cooling budget of the dilution refrigerator, and the expected heat load on the sub-Kelvin cryostat layers (for the baseline design) are provided in the table within figure 10.

The C-stems require flexibility in all three directions. In the longitudinal direction, the stems will shrink nearly 0.3% of their length when cooled from room temperature to the base cryogenic temperature. For ~10 feet length, the shrinkage is ~9 mm. The flexibility requirement in the transverse direction comes from the hanger arrangement of the sub-Kelvin layers. Each layer is hung using thermally insulating thin Kevlar strings from the outer layer, and this assembly is prone to swinging in the tranverse direction in case of ground motion (Note that the experiment will be housed in an active underground mine in Sudbury, Canada where rock blasting can produce ground motion). While it is difficult to predict the level of motion expected in this scenario, a few mm of flexibility may be adequate to compensate the transverse motion of the cryostat layers. Flexibility in the vertical direction is for providing a few mm motion in this direction as the cryostat layers and C-stems settle into their final design positions after cooldown (the components are assembled with a vertical offset at room temperature such that they will move during cooldown and align into their operating design following thermal contraction during cooldown). Due to the multi-directional flexibility need, FTLs made of strand-woven copper cables (Technology Applications, Inc. UltraFlex PT502) for the C-stem were chosen for the experiment. An example connection is shown in figure 10, which has two copper cable FTLs connecting the MC C-stem parts. As discussed in Section 3, thermal conductance of the off-the-shelf FTL was inadequate below 1 K and was subsequently improved by e-beam welding the FC to EC's. The reader is directed to [22] for further details of the SuperCDMS SNOLAB sub-Kelvin cryo-system.

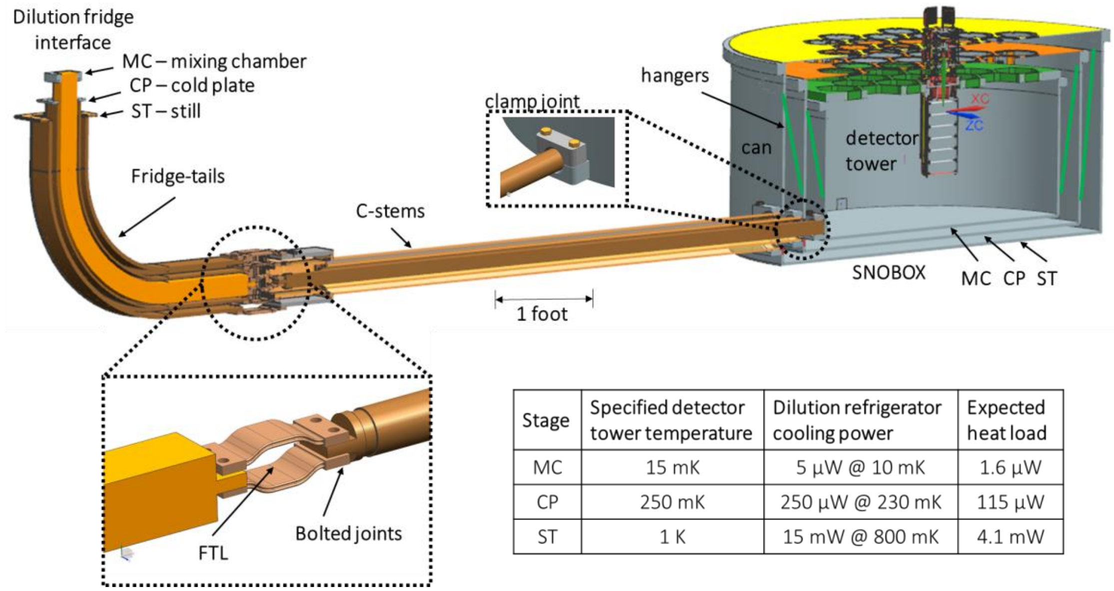

Stage	Specified detector tower temperature	Dilution refrigerator cooling power	Expected heat load
MC	15 mK	5 μW @ 10 mK	1.6 μW
CP	250 mK	250 μW @ 230 mK	115 μW
ST	1 K	15 mW @ 800 mK	4.1 mW

Figure 10. Baseline design of the sub-Kelvin architecture of the SuperCDMS SNOLAB experiment in which a three layered copper enclosure is conduction-cooled by a dilution refrigerator using tubular OFHC copper thermal buses and copper cable FTLs [22].

b) Cryocooler conduction-cooled SRF cavities

Fermi National Accelerator Laboratory is developing cryocooler conduction-cooled superconducting radiofrequency (SRF) cavities for use in particle accelerators. It is anticipated that by eliminating reliance on large quantities of liquid helium that conventional SRF cryo-systems require, this cryogen-free technique will make the SRF accelerator technology more accessible to researchers and to the particle accelerator industry. This draws parallel with superconducting magnet (SCM) technology that in early days relied on liquid helium but is now commercially available with cryogen-free cryo-systems.

Note that conduction-cooling for SRF is much more demanding in terms of the required thermal conductance than for a SCM. This is because SRF cavities contain heat dissipative electromagnetic fields unlike non-dissipative DC fields in SCMs. For example, the 5-cell SRF cavity being developed at Fermilab is expected to dissipate ~10 W at 5 K, which is an order of magnitude higher than a typical conduction-cooled SCM.

A working design of conduction-cooling scheme for the Fermilab SRF niobium cavity is depicted in figure 11. Firstly, niobium rings are welded on the elliptical cells near the equator to provide a flat surface for connecting the thermal link. The link is made of 5N aluminum (>99.999% pure) and comprises of the following: conduction rings that bolt to the niobium rings on the cells, four ear straps per cell spaced at 90 degrees azimuthally, four thermal buses extending over the cavity length and spaced at 90 degrees azimuthally, and an FTL on each bus ultimately connecting to the cryocooler 4 K stage. Four Cryomech PT420 coolers operating at ~4.5 K are required to balance the ~10 W @ 5 K cavity heat dissipation. The thermal link needs to transport 10 W of heat with a temperature drop of <0.5 K.

Of the allowable 0.5 K, the FTL was designed to exhibit <0.15 K temperature difference while transporting 2.5 W of heat, which in terms of thermal conductance is nearly >17 W/K. The thermal link and cavity support are designed such that the differential thermal contraction between the cavity (niobium) and thermal bus (aluminum) is compensated by U-bend of the ear strap. The FTL has to only provide ~5 mm motion in the longitudinal direction. Due to this unidirectional flexibility requirement, stacked foil geometry was selected for the FTL. The stack has thirty foils of 5N aluminum, each foil being 0.5 mm thick, 75 mm wide, and 10 cm long. The stack is then placed between machined ECs of 5N aluminum and e-beam welded together to minimize FC-EC contact resistance. Going by the measured thermal conductivity of the 0.5 mm thick 5N aluminum foils (Al-1 in figure 2), we expect that the FTL will have thermal conductance of ~22 W/K.

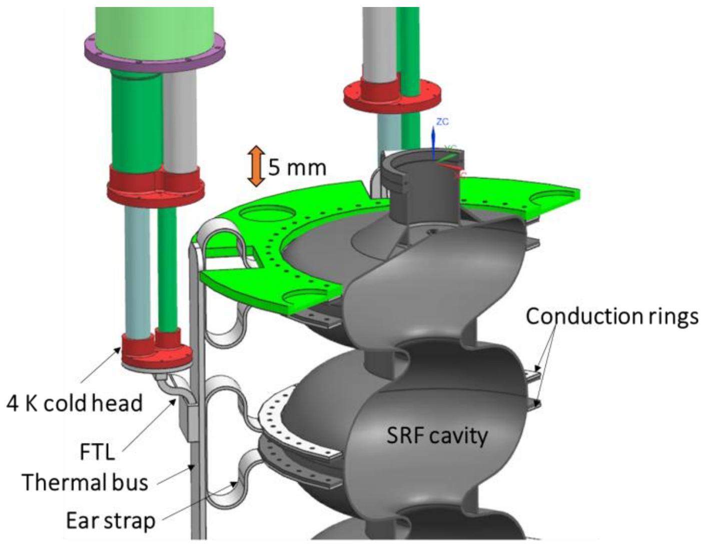

Figure 11. CAD rendering of the cryocooler conduction-cooled SRF cavity being developed at Fermi National Accelerator Laboratory. For prototype cavity performance, see [23,24].

7. Resources

Information on commercial FTL suppliers is available on the Cryogenic Society of America's website: https://csabg.org/thermal_straps/. These suppliers provide off-the-shelf and custom FTLs as well as thermal and structural characterization services.

8. Acknowledgement

This manuscript has been authored by Fermi Research Alliance, LLC under Contract No. DE-AC02-07CH11359 with the U.S. Department of Energy, Office of Science, Office of High Energy Physics.

9. References

1. D. Bugby and B. Marland. 2003. Flexible conductive links. pp. 327 – 346. *In*: M. Donabedian [ed.]. Spacecraft Thermal Control Handbook, Volume II: Cryogenics. The Aerospace Press. El Segundo, California, USA.

2. S. Nakamura, D. Miyafuji, T. Fujii, T. Matsui and H. Fukuyama, “Low temperature transport properties of pyrolytic graphite sheet”, Cryogenics 86, 118–122, 2017.

3. S. Nakamura (University of Tokyo, Japan), personal communication.

4. A. Hauser and S. Dolce, “Design concepts for flexible thermal links” SAE Transactions 105 Section 1: Journal of Aerospace, 556 – 562, 1996.

5. Thermal conductivity of aluminum, copper, iron, and tungsten for temperatures from 1 K to the melting point, NBSIR 84-3007.

6. I.M. McKinley, C.H. Smith, P.G. Ramsey and J.I. Rodriguez, “Pyrolytic graphite film thermal straps: Characterization testing”, Cryogenics 80(1), 174 – 180, 2016.

7. F. Pobell, “Matter and methods at low temperature”, Springer Berlin, Heidelberg (3rd edition), 2007.

8. A.L. Woodcraft, “Recommended values for the thermal conductivity of aluminium of different purities in the cryogenic to room temperature range, and a comparison with copper”, Cryogenics 45(9), 626 – 636, 2016.

9. R.C. Dhuley, M. Ruschman, J.T. Link and J. Eyre, “Thermal conductance characterization of a pressed copper rope strap between 0.13 K and 10 K”, Cryogenics 86, 17 – 21, 2017.

10. R.C. Dhuley, R. Kostin, O. Prokofiev, M.I. Geelhoed, T.H. Nicol, S. Posen, J. C. T. Thangaraj, T. K. Kroc, and R. D. Kephart, “Thermal link design for conduction cooling of SRF cavities using cryocoolers”, IEEE Transactions on Applied Superconductivity 29(5), 0500205, 2019.

11. M.O. Kimball and P.J. Shirron, “Ultra-flexible thermal bus for use in the Astro-H Adiabatic Demagnetization Refrigerator”, GSFC-E-DAA-TN24452, 2017.

12. M.O. Kimball, (NASA Goddard Space Flight Center, USA), personal communication.

13. T. Yamada, T. Tomaru, T. Suzuki, T. Ushiba, N. Kimura, S. Takada, et al., “High performance heat conductor with small spring constant for cryogenic applications”, Cryogenics 116, 103280, 2021.

14. L. Risegari, M. Barucci, E. Olivieri, E. Pasca and G. Ventura, “Measurement of the thermal conductivity of copper samples between 30 and 150 mK”, Cryogenics 44(12), 875 – 878, 2004.

15. T. Trollier, J. Tanchon, J. Lacapere, P. Renaud, J.C. Rey and A. Ravex. "Flexible Thermal Link Assembly Solutions for Space Applications", Cryocoolers 19, 595-603, 2016

16. S-bond solder, https://www.s-bond.com/applications-2/pyrolytic-graphite-thermal-management/, 2020.

17. M.I. Hollister, D.A. Bauer, R.C. Dhuley, P. Lukens, L.D. Martin, M.K. Ruschman, R.L. Schmitt and G.L. Tatkowski, "The cryogenics design of the SuperCDMS SNOLAB experiment", IOP Conference Series: Materials Science and Engineering 278, 012118, 2017.

18. W. Stautner, E. Budesheim and R. Chen, "Use of Galinstan as a Contact Agent for Additively Manufactured Components in Cryogenic Engineering", IOP Conference Series: Materials Science and Engineering 755, 012119, 2020.

19. E. Gmelin, M. Asen-Palmer, M. Reuther and R. Villar, "Thermal boundary resistance of mechanical contacts between solids at sub-ambient temperatures", Journal of Physics D: Applied Physics 32(6), R19, 1999.

20. R.C. Dhuley, "Pressed copper and gold-plated copper contacts at low temperatures – A review of thermal contact resistance", Cryogenics 101, 111–124, 2019.

21. R.C. Dhuley, M.I. Geelhoed and J.C.T. Thangaraj, "Thermal resistance of pressed contacts of aluminum and niobium at liquid helium temperatures", Cryogenics 93, 86 – 93, 2018.

22. R. C. Dhuley, M. I. Hollister, M. K. Ruschman, L. D. Martin, R. L. Schmitt, G. L. Tatkowski, D. A. Bauer, and P. T. Lukens, "Thermal conductance modeling and characterization of the SuperCDMS SNOLAB sub-Kelvin cryogenic system", IOP Conference Series: Materials Science and Engineering 278, 012157, 2017.

23. R. C. Dhuley, S. Posen, O. Prokofiev, M. I. Geelhoed, and J. C. T. Thangaraj, "First demonstration of a cryocooler conduction-cooled superconducting radiofrequency cavity operating at practical cw accelerating gradients", Superconductor Science and Technology 33, 06LT01, 2020.

24. R.C. Dhuley, S. Posen, M.I. Geelhoed, and J.C.T. Thangaraj, "Development of a cryocooler conduction-cooled 650 MHz SRF cavity operating at ~10 MV/m cw accelerating gradient", IOP Conference Series: Materials Science and Engineering 1240 (1), 012147, 2022.